AJNR

Imaging findings and MRI patterns in a cohort of 18q chromosomal abnormalities

Prateek Malik, Helen Branson, Grace Yoon, Manohar Shroff, Susan Blaser and Pradeep Krishnan

AJNR Am J Neuroradiol published online 30 May 2024
http://www.ajnr.org/content/early/2024/05/30/ajnr.A8361

Published May 30, 2024 as 10.3174/ajnr.A8361

ORIGINAL RESEARCH

Imaging findings and MRI patterns in a cohort of 18q chromosomal abnormalities

Prateek Malik, Helen Branson, Grace Yoon, Manohar Shroff, Susan Blaser[¥], Pradeep Krishnan[¥]

ABSTRACT

BACKGROUND AND PURPOSE: The abnormalities of long arm of chromosome 18 (18q) constitute a complex spectrum. We aimed to systematically analyze their MRI features. We hypothesized that there would be variable but recognizable white matter and structural patterns in this cohort.

MATERIALS AND METHODS: In this retrospective cohort study, we included pediatric patients with a proven abnormality of 18q between 2000-2022. An age and sex matched control cohort was also constructed.

RESULTS: Thirty-six cases, median MRI age 19.6 months (4.3 – 59.3), satisfied our inclusion criteria. Majority were females (25, 69%, F:M ratio 2.2:1). Fifty MR imaging studies were analyzed and 35 (70%) had delayed myelination. Two independent readers scored brain myelination with excellent interrater reliability. Three recognizable evolving MRI patterns with distinct age distributions and improving myelination scores were identified – PMD-like (9.9 months, 37), intermediate (22 months, 48) and washed-out pattern (113.6 months, 53). Etiologically, MRIs were analyzed across three subgroups - 18q- (34, 69%), trisomy 18 (10, 21%) and ring chromosome 18 (5, 10%). Ring chromosome 18 had the highest myelination lag (27, P value = 0.005) and multifocal white matter changes (P value = 0.001). Trisomy 18 had smaller pons and cerebellar dimensions (APD pons P value = 0.002, CC vermis P value <0.001 and TCD P value = 0.04).

CONCLUSIONS: In this cohort of 18q chromosomal abnormalities, MRI revealed recognizable patterns correlating with improving brain myelination. Imaging findings appear to be on a continuum with more severe white matter abnormalities in ring chromosome 18 and greater prevalence of structural abnormalities of pons and cerebellum in trisomy 18.

ABBREVIATIONS: 18q-: 18q deletion; CC: corpus callosum; CC-APD: CC anteroposterior diameter; FOD: fronto-occipital diameter; TCD: transverse cerebellar diameter; APD: anteroposterior diameter; CCD: craniocaudal diameter; MBP: myelin basic protein; PMD: Pelizaeus-Merzbacher Disease; GWMD: gray-white matter differentiation

Received month day, year; accepted after revision month day, year..
From the Department of Department of Diagnostic Imaging, The Hospital for Sick Children, Toronto, Canada (P.M., H.B., M.S., S.B., P.K.) and Division of Clinical & Metabolic Genetics, The Hospital for Sick Children, Toronto, Canada (G.Y.).

¥ - indicates co-senior authors

The authors declare no conflicts of interest related to the content of this article.

Please address correspondence to Pradeep Krishnan, Department of Diagnostic Imaging, The Hospital for Sick Children, Toronto, Canada, 170 Elizabeth St, Toronto, ON M5G 1E8, pradeep.krishnan@sickkids.ca

SUMMARY SECTION

PREVIOUS LITERATURE: Genetic disorders affecting the long arm of chromosome 18 (18q) are heterogenous. These can variably affect the zygosity of genetic material including suprazygosity or duplicated genetic material (trisomy or tetrasomy 18) and hemizygosity or missing genetic material (18q deletion or 18q-, ring chromosome 18). Recent advancements have led to creation of gene dosage maps to narrow down clinical phenotypes to the affected chromosome 18 segment and zygosity state. Even though imaging findings are well studied in the 18q-, similar MRI correlates are not well established mainly due to limited cohort data regarding MRI phenotypes across other genetic disorders affecting 18q.

KEY FINDINGS: Three discernible MRI patterns suggesting age-evolving myelination phenotypes were noted across the 18q spectrum. A diverging spectrum of MRI changes emerged across the 18q subgroups with most pronounced white matter changes (highest myelination lag, multifocal white matter changes) in ring chromosome 18, and significantly reduced pons and cerebellar biometry in trisomy/tetrasomy 18.

KNOWLEDGE ADVANCEMENT: Our results indicate a particular vulnerability of pons and cerebellum in suprazygous chromosome 18 states, white matter susceptibility (with pons and cerebellar sparing) in ring chromosome 18, and intermediate changes in 18q-. These results may offer insights into understanding complex mechanisms and gene dosage effects in these disorders.

INTRODUCTION

Abnormalities of the long arm of chromosome 18 (18q) constitute a spectrum of clinical and imaging phenotypes and are amongst the

Copyright 2024 by American Society of Neuroradiology.

commonest chromosomal abnormalities. [1] The long arm can get affected through complex mechanisms including and not limited to duplication (trisomy or tetrasomy 18) or deletion (18q deletion or 18q-, ring chromosome 18) of particular segments or in entirety. These typically lead to abnormalities across multiple organ systems, including the CNS, affecting each to a variable degree. Affected individuals can exhibit a uniquely affected long arm with variations in the length (from a single gene to large segments) and location of the involved segments rendering highly variable and diverse phenotypes.(2)

There has already been a perceptible shift in research and clinical practice towards recognizing the effects of these alterations at a genetic level to better define the clinical phenotypes with predictive outcomes. Individually, the genes on the 18q have diverse biological roles, may be dosage sensitive and thus may be variably affected from hemizygosity (missing genetic material including deletions) or suprazygosity (duplicated genetic material including trisomy, tetrasomy). [3] This has led to creation of gene dosage maps (https://wp.uthscsa.edu/chrome-18/research/) in an attempt to narrow down phenotypes to specific genes or select regions of chromosome 18 and classified according to states of zygosity. [4,5]

This has renewed the interest in understanding the imaging changes in this group of disorders collectively. Imaging findings from CNS involvement are highly variable ranging from white matter abnormalities to malformative changes including commissural hypoplasia, migrational defects, hydrocephalus, porencephaly, cerebellar hypoplasia, pituitary abnormalities and microcephaly . [1,6–8] Studies examining comparative differences across these disorders are sparse in the current literature. Systematic analysis of imaging remains limited to 18q- cohorts with limited MRI descriptions of the other abnormalities. [9–15]While white matter changes are well-described in 18q- , proposed due to delayed myelination from myelin basic protein (MBP) gene haploinsufficiency with a possible yet undefined role of some other potential genes [1], these remain poorly characterized across the rest of the 18q spectrum largely due to smaller cohort numbers. [13–15]

We aimed to systematically analyze MRI features across a cohort of cases with abnormalities involving the long arm of chromosome 18 including deletion, trisomy, tetrasomy, inversion and ring chromosome 18 with particular attention to white matter abnormalities as well as malformative features. We also hypothesized that there would be temporally evolving myelination patterns with age in this cohort and the white matter would be variably affected across the 18q spectrum.

MATERIALS AND METHODS

This research ethic board (REB) approved single center study retrospectively recruited children with abnormalities affecting the long arm of chromosome 18 over a period of 22 years (2000-2022) through a search of the electronic medical records. The inclusion criteria were: 1) Age between 0-18 years 2) confirmed abnormality of long arm of chromosome 18 with karyotype analysis 3) MRI with at least a T1 and T2 weighted sequence, performed at any time during the course of illness.

Clinical findings were documented when available. MR imaging was performed on either 1.5T or 3T MRI scanners. Signal characteristics were assessed on axial fast spin-echo T2 and axial gradient-echo T1 weighted images. We leveraged a previously described 18-region age-appropriate myelination scoring system to systematically assess cerebral, cerebellar and brainstem myelination and calculated T1 and T2 myelination scores using standardized definitions.[16,17] Individual structures were scored as 0 (lack of myelination) to 2 (complete myelination) and total scores deviating by more than 2 from age-expected scores were rated as abnormal. [16] These were independently assessed by two fellowship trained pediatric neuroradiologists (P.M., P.K. with 4- and 12-year neuroradiology experience respectively) and interrater reliability (IRR) was assessed for T1 and T2 scores for each structure and the total myelination score. To further qualitatively assess the white matter changes, dominant myelination patterns were discerned and compared for T1, T2, total myelination scores and myelination lag (expected myelination score – total myelination score). We analyzed differences between age distribution, changes in biometric and myelination score parameters across the patterns.

The MRIs were additionally reviewed in consensus for regions with focal signal changes. We also compared the definition and thickness of the peripheral cerebellar white matter stripes on T1 sagittal images (Online Supplemental Data) at the level of the trigone to age matched controls in the cases older than 18 months of age, when an adult-expected pattern is reached. [18]

For biometric measurements, two-fellowship trained neuroradiologists conducted an initial pilot review of 10 cases to establish standardization in application of biometric measurement criteria and as an excellent agreement has demonstrated for these measurements across multiple prior studies [19–21], subsequent measurements performed by consensus review of cases. The corpus callosum (CC) was assessed quantitatively using standardized methods including the CC anteroposterior diameter (CC-APD) and thickness of CC segments (genu, body and splenium). [19] To produce normalized ratios, fronto-occipital diameter (FOD) was also measured. [19] Brainstem and cerebellar measurements including pons AP diameter (APD pons), craniocaudal diameter (CCD) vermis and transverse cerebellar diameter (TCD) were also collected using standardized methods. [20,21] The corpus callosum, brainstem and cerebellar biometry were compared to age-matched reference data, considered small when <3rd centile. [16,19,20] An age and sex matched control cohort was also constructed using MRIs of developmentally intact children with normal imaging for comparison of the biometric parameters.

Statistical analysis and data visualization was performed using SPSS version 25 and Python 3.7.8. Data from the collected variables were assessed for normality using the Shapiro-Wilk test. Statistical differences across parametric and non-parametric continuous variables were assessed using one way ANOVA and Kruskall-Wallis tests respectively and adjusted with post-hoc analysis for multiple comparison tests as necessary. [22] The chi square and Fisher exact tests were used for analysis of categorical data and Wilcoxon signed-rank test was used for comparison with the control group. [23] IRR was measured using intraclass correlation coefficient (ICC) calculated via a two-way mixed model based on absolute agreements, and standardized cut-offs for levels of agreement were used. [24] All statistical tests were 2-sided, and statistical significance was assumed at P value of .05.

RESULTS

Thirty-six cases satisfied our inclusion criteria (Table 1). Out of these, 18q- formed the largest group (23 cases, 64%). Median age at MRI was 19.6 months (4.3 – 59.3) and majority were females (25, 69%, F:M ratio 2.2:1). Availability of clinical data and documentation were variable, available for less than half of the cases as detailed.

Fifty MRI studies from 36 cases were analyzed (Table 1). Thirty-three out of the 36 cases (92%) had at least 1 abnormal MRI. Abnormal white matter was the commonest abnormality, present in 70% (35 MRIs). Structurally, corpus callosum abnormalities were the most

common finding, noted in 60% (30 studies) followed by small CCD vermis dimension (14 studies, 28%) and small APD pons (10 studies, 20%).

Control Cohort comparison

Biometric measurements were also obtained from an age and sex matched control cohort of 100 cases (median age 45.4 months, 13.4 – 111.2, Online Supplemental Data). All biometric measurements pertaining to the corpus callosum, pons and cerebellar dimensions were significantly smaller than the controls (P value </=0.001). FOD measurements were also significantly smaller in the 18q group. As smaller head dimensions could have had confounding effects on the brainstem and cerebellar biometry, the data was normalized by obtaining FOD ratios. The normalized ratios were smaller but not significantly different from the control group.

Myelination Scoring and pattern assessment

Fifteen (30%) MRIs had an age-appropriate appearance of the white matter. The signal changes in the remaining 35 MRIs (70%) had white matter abnormalities consistent with a delayed myelination pattern but were different across the cohort. Additionally, scattered multifocal foci of FLAIR hyperintensity (not compatible with the described MRI patterns) were noted in 4 MRIs (8%, age range 15.2 – 199.6 months, median, IQR 198.3, 106.1 – 213.5 months). We could identify three dominant patterns (Fig 1) which were defined as follows: 1) Pelizaeus-Merzbacher Disease (PMD)-like pattern where myelination was diffusely and homogenously lacking with a homogenously hyperintense T2 white matter signal change. In this pattern, the gray-white matter differentiation (GWMD) was preserved and could be defined in all regions; 2) Intermediate-pattern: where there was a dirty heterogenous white matter signal, often having a dot-like appearance with inhomogeneous GWMD and mixed areas of preserved and loss of GWMD; 3) Washed-out pattern where the T2 hyperintensity was milder and the GWMD was diffusely poor.

For myelination scoring, there was excellent agreement between the readers with all ICC scores >0.75 (Online Supplemental Data). The analysis revealed distinct age distributions of the patterns suggesting a temporally evolving myelination phenotype with the youngest cases having a PMD-like pattern (8 MRIs, 16%, median age: 9.9 months) and the oldest in the washed-out pattern (17 MRIs, 34%, median age: 113.6 months, Online Supplemental Data) with significantly and temporally improving T1, T2 and total myelination scores. There remained a median myelination lag of 18 points in comparison to age-matched controls which was worst in the intermediate-pattern group (age range 15.4 – 49 months). Corresponding to improving myelination, significant temporal improvements were also noted in the corpus callosum, pons and cerebellar biometry across the three patterns (Online Supplemental Data).

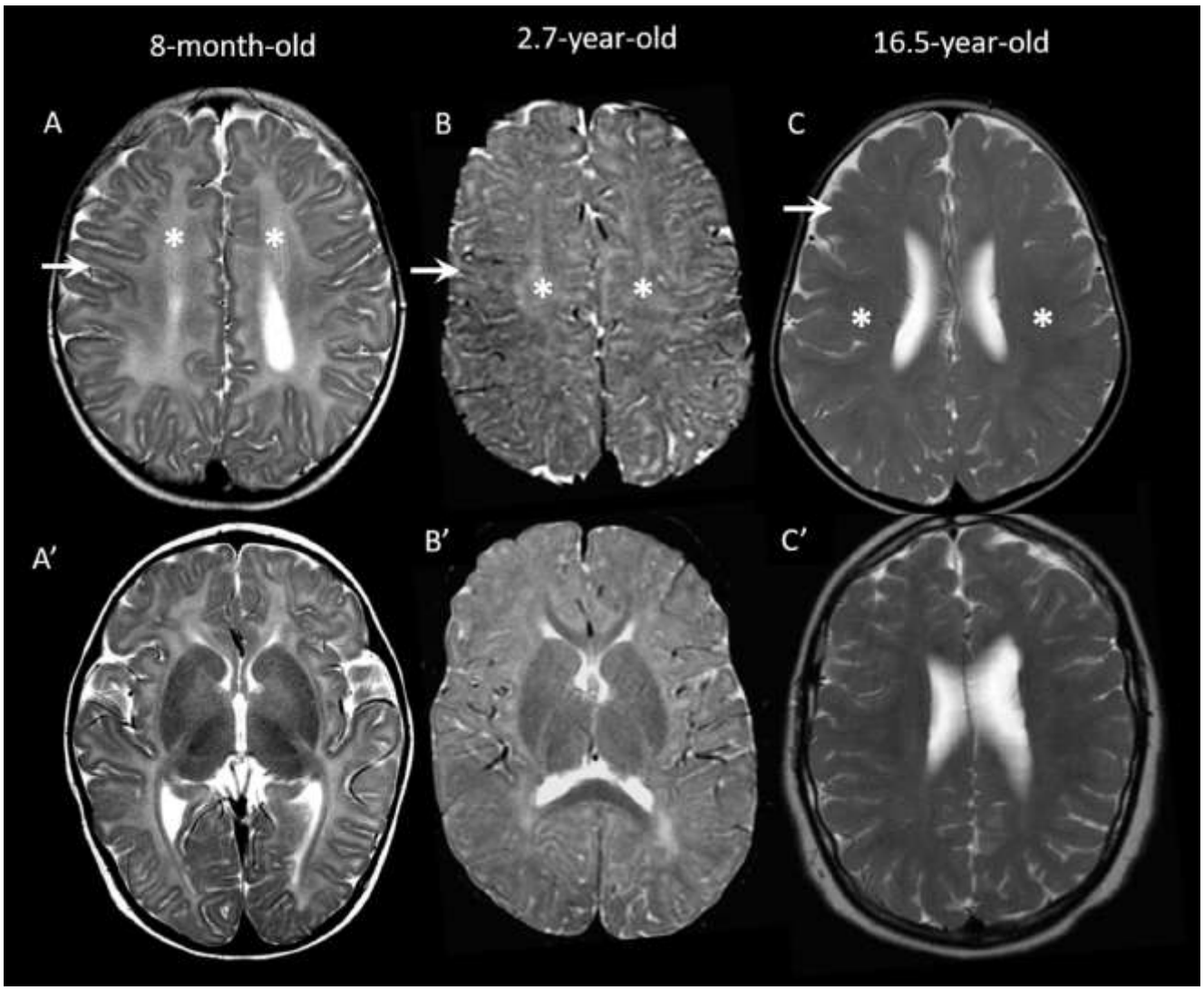

Fig 1. MRI patterns in three different cases. Images A, A' show a PMD-like pattern with diffuse T2-hyperintensity of white matter (asterisk A) and preserved GWMD (arrow A). Images B, B' show the "intermediate pattern" with mixed areas of preservation and loss of GWMD (arrow B) with dirty inhomogeneous white matter appearance (asterisk B). Images C, C' show the "washed-out pattern" with milder diffuse

abnormal signal (asterisk C) with diffusely poor GWMD (arrow C).

Analysis of focal signal changes

The closed eye sign of medial lemniscus (Fig 2), described in literature as a better myelinated T2 hypointense medial lemniscus than the surrounding structures [25] and also seen transiently during normal myelination of brainstem [26], was seen in 9 (18%) studies and more commonly with the PMD-like pattern (Online Supplemental Data). A mild focal T2 hyperintensity involving the middle blade of splenium at the midline (Fig 2) was seen in 3 cases (1 each in three patterns) and was only mildly T1 hypointense. Poor cerebellar white matter arborization with less robust peripheral stripes and T1 signal (Online Supplemental Data) was found in 26 (53%) MRIs, majority in the washed-out pattern (16, 94%). In 6 (35%) of the washed-out pattern MRIs, an accentuated T2 hyperintensity was noted in the occipital lobes and posterior limb of internal capsule.

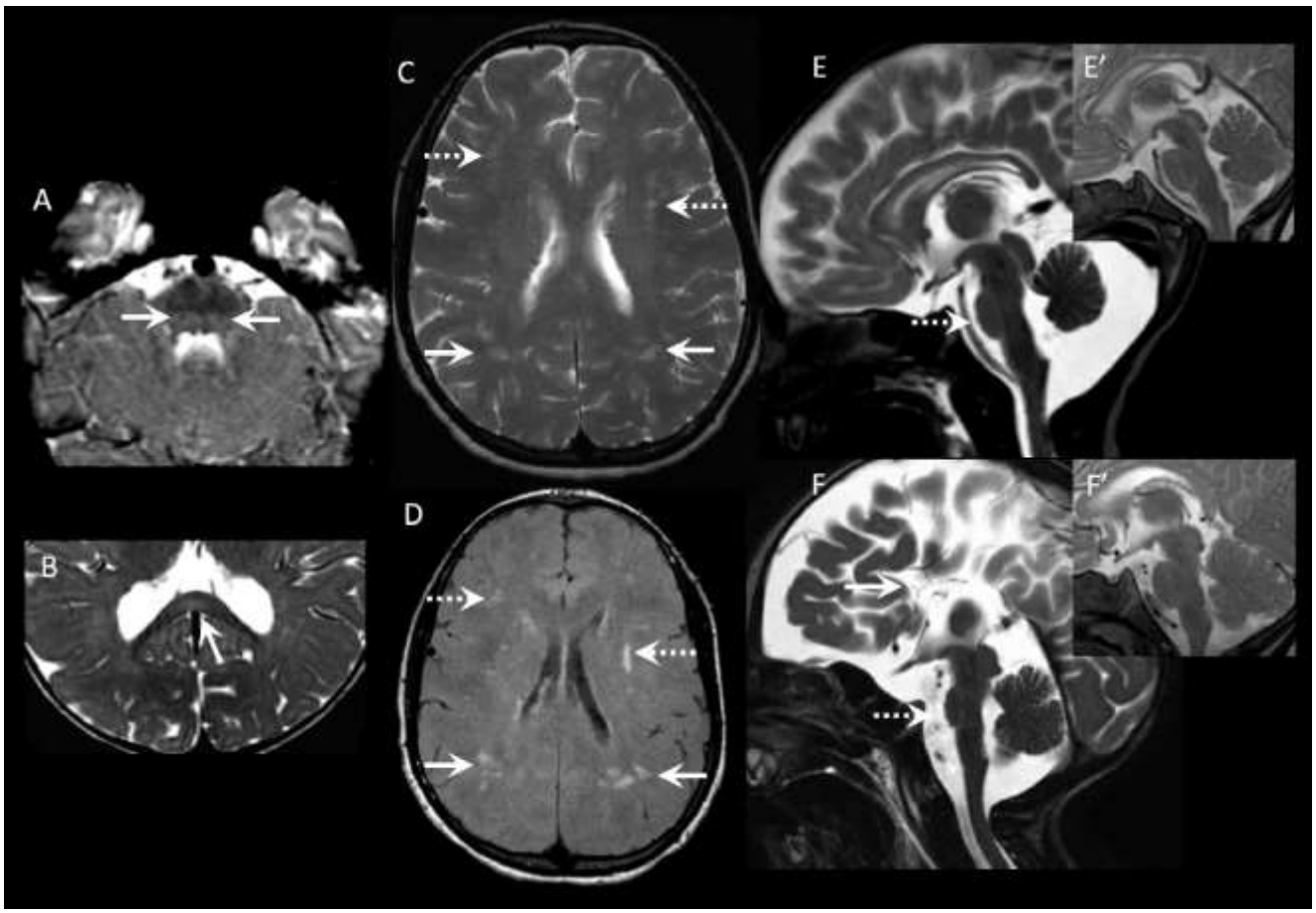

Fig 2. Focal signal changes and small pons. Axial T2 images show relatively better myelination and T2 hypointensity of the medial lemniscus (arrows, A) in the dorsal brainstem (closed eye sign) and focal mid-splenial T2 hyperintensity (arrow, B). Axial T2 (C) and FLAIR(D) images in an 18-year-old with ring chromosome 18 show multiple scattered focal hyperintensities in the frontal (dashed arrows) and parietal (solid arrows) white matter in the background of a washed-out MRI pattern. Midline sagittal sections in two trisomy 18 cases at 1 and 3 months (E,F respectively) showing a reduced APD of pons and agenesis of corpus callosum in case 2 (arrow, F). Normal appearance of the pons in age-matched controls provided for reference in the inset images (E',F').

Cases with follow-up MRI

Eleven cases in our cohort had at least 1 follow-up MRI with a total 25 MRIs and an average of 2.2 MRI studies (25 MRIs /11 case). Nine cases had 18q- and 1 case each had 18 tetrasomy and ring chromosome 18. An age-expected final myelination score (i.e. myelination lag of 0) was attained in only two children, 1 each with 18q- and 18 tetrasomy. In the other 9 children, an average final myelination lag of 14.8 points remained at follow-up.

All 11 cases with a follow-up study showed myelination progression (increase in myelination score) on the follow-up MRI. Amongst these, 7 cases (64%, average age at MRI 109 months) showed a decreasing myelination lag (age-expected myelination score – patient myelination score) or partial "myelination catch-up" on follow-up while 4 cases (36%, average age at MRI 101 months) showed an increase in myelination lag (failure of "myelination catch-up") on follow-up despite myelination score progression.

Comparative analysis of 18q subgroups

Three groups were analyzed – 18q- (23, 34 MRIs), ring chromosome 18 (4, 5 MRIs) and trisomy 18 (8, 10 MRIs) group (Table 2, expanded table in Online Supplemental Data). A single case of tetrasomy 18 was assessed together with the 7 trisomy 18 cases. A single case of 18q inversion was excluded from the subgroup analysis as this was the only case and there were complex changes in the genetic material. Ring chromosome 18 group had the highest prevalence of white matter abnormalities (5, 100%), though this was not significantly different from other groups. Ring chromosome 18 also had significantly higher prevalence of multifocal white matter changes (3, 60%, P value = 0.001) and the highest levels of myelination lag (27, P value = 0.005, 0.03 vs trisomy 18, 18q- groups respectively). Corpus callosum abnormalities and dimensions were not significantly different. Cerebellar and pons biometry however, including APD pons, CCD vermis and TCD, were all significantly smaller in the trisomy 18 group (P values = 0.002, <0.001, 0.04 respectively). These were also smaller than the 3rd centiles for age-referenced data for trisomy 18 group. FOD normalized ratios for pons and vermis, including APD pons/FOD and CCD vermis/FOD, remained significantly smaller indicating an effect independent to an overall smaller head size. There were no significant differences between MRI patterns across the groups.

Core imaging features and 18q subgroups

Based on the above analysis, 4 core features were noted (delayed myelination, multifocal white matter changes, small pons, small vermis) and their distribution and overlaps in the 18q-, ring chromosome 18 and trisomy 18 groups was assessed and represented with respective Venn diagrams (Fig 3, Table 3). In the 18q- group, 30/34 MRIs had at least one of the core features. Amongst these, majority had isolated delayed myelination (21/30, 70%) or delayed myelination with a small pons and/or a small vermis (4/30). Five cases of 18q- had an isolated small vermis or small pons. In trisomy 18 group, all MRIs had at least one of the core features (10, 100%) and a small pons and/or a small vermis were almost always present (9, 90). None of the ring chromosome 18 MRIs had a small pons or vermis, and delayed myelination was present in all (5,100%), either in isolation (2, 40%) or with multifocal white matter abnormalities (3, 60%).

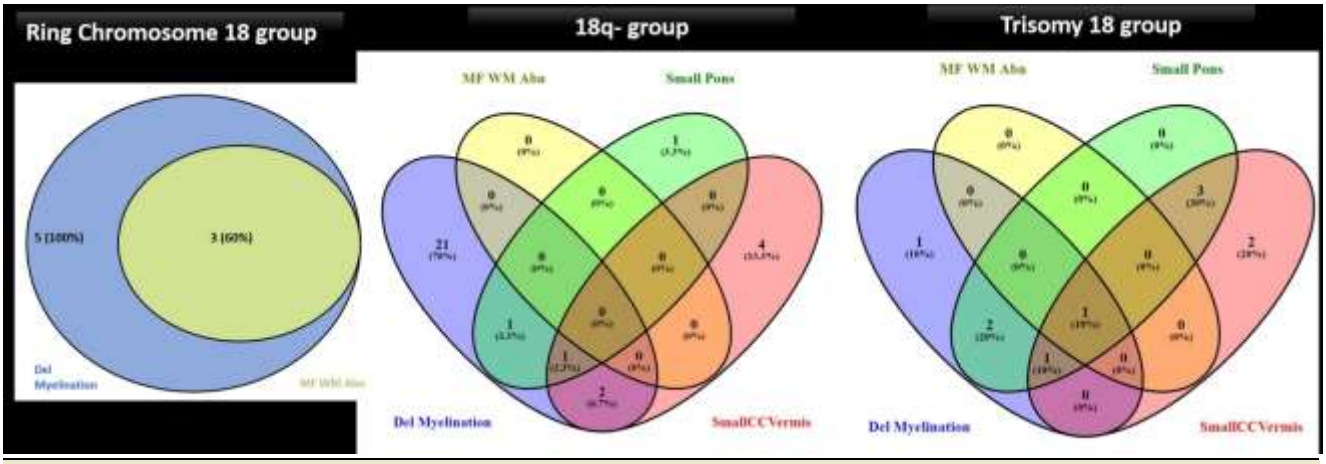

Core Features	Ring Chromosome 18	18q deletion (18q-)	Trisomy/tetrasomy 18
1. Delayed Myelination	+++	++	++
2. Multifocal white matter changes	++	-	+
3. Small pons (APD pons <3rd centile)	-	+	+++
4. Small vermis (CCD vermis <3rd centile)	-	+	+++

Fig 3 and Table 3. Venn diagram and table detailing MRI core feature distribution across etiology subgroups (90% or greater: +++; 50-70%: ++; <20%: +)

DISCUSSION

In this retrospective cohort study of 50 MRIs from 36 cases with 18q abnormalities, 3 evolving MRI patterns of delayed myelination with distinct age distributions and progressing myelination scores were identified – PMD-like (9.9 months, 37), intermediate (22 months, 48) and washed-out pattern (113.6 months, 53; P value = 0.01) with temporally improving corpus callosum, pons and cerebellar dimensions. Myelination and structural changes were on a spectrum across the three 18q subgroups. Most severe white matter involvement with the highest myelination lag (27, P value = 0.005 vs trisomy 18, 0.03 vs 18q-) and multifocal white matter changes (P value = 0.001) were noted in the ring chromosome 18 subgroup, while the most advanced cerebellar and pontine hypoplasia was noted in the trisomy 18 subgroup (APD pons P value = 0.002, CCD vermis P value < 0.001 and TCD P value = 0.04) independent of effects from a smaller head size. The distribution of the core imaging features including delayed myelination, multifocal white matter changes, small pons and vermis were elaborated for the main etiology subgroups.

Within the 18q disorders, MRI findings remain better characterized in the 18q- group, especially white matter abnormalities. In our cohort,

white matter abnormality was consistent with a delayed myelination appearance with the prevalence of 74% (25 MRIs) in 18q- cohort in keeping with the range of 50-71% in literature [6,8,27,28] except for 95% in a single study where majority of the cases had MBP haploinsufficiency.[29] There is little consensus however on the dominant conventional MRI pattern in literature with variable descriptions including a central deep white matter predominant pattern [8] or diffusely poor myelination pattern with a poor GWMD. [28] Occasional cases with severe myelin deficit have also been described. [8,27,28] Based on this knowledge that the myelination phenotype may be markedly different and may vary with age, we were able to divide the MRI studies into three recognizable phenotypes - PMD-like, intermediate and washed-out patterns. This has diagnostic utility as imaging appearances in 18q abnormalities can be similar to Pelizaeus-Merzbacher disease during the first year,[30] corresponding to age range of the PMD-like phenotype (3-12 months). Consistent with some of the quantitative imaging studies using myelin water fraction and MRI relaxometry techniques, [1,7,29] we found these patterns corresponded to improving myelination scores. The final myelination phenotype seemed to be the washed-out pattern after which there was no further decrease in myelination lag, consistent with the final equilibrium levels described with quantitative studies. [1,7,29]

There are anecdotal reports of MRI findings in ring chromosome 18 in literature, and most descriptions in trisomy 18 remain restricted to autopsy reports.[11,13–15] We found a delayed myelination phenotype in all cases with ring chromosome 18 with the highest levels of myelination lag (P value = 0.005, 0.03 vs trisomy 18, 18q- groups) and multifocal white matter abnormalities (P value = 0.001). This is consistent with reports in literature with more severe white matter findings in comparison to 18q-.[13] Evidence from autopsy reports suggests that CNS changes in trisomy 18 are more commonly structural with a wide spectrum, most pertinently including hypoplasia of pons, cerebellum (~90%).[31] To best of our knowledge, while white matter changes in trisomy 18 have been described in a few cases on autopsy, [32,33] these seem remain poorly characterized on MRI. Similar to the prevalence described in literature,[31] a small pons and/or vermis was present in almost all trisomy 18 MRIs (9, 90%). Delayed myelination was seen in 50% (5) with only 1 MRI having an isolated delayed myelination without a small pons or vermis. Interestingly, none of the ring chromosome 18 cases had a small pons or vermis. In contrast to ring chromosome 18 and trisomy 18 subgroups, 18q- had an isolated delayed myelination in 21 MRIs (62%), 5 MRIs (18%) with isolated small pons and/or vermis and rest 10 (20%) with overlapping delayed myelination, small pons and/or vermis. This presence of mixture of structural and white matter changes of varying severity in 18q- are in keeping with the autopsy reports.[34,35] It is tempting to speculate if the imaging findings in ring chromosome 18, 18q- and trisomy 18 thus represent a continuum of structural and white matter changes. Future larger cohorts are needed to assess this further.

In some cases, we found regionally specific myelination delays. This included some cases with focal mid splenial T2 hyperintensity which was only mildly T1 hypointense and we speculate this represents an appearance related to delayed mid splenial myelination. The splenium follows a centrolineal pattern of myelination and can have variable signal centrally from 3-6 months as a normal developmental phenomenon. [36] A similar finding has also been described in 4H leukodystrophy, however with a T1-hypointense cyst-like appearance, assumed to represent tissue rarefaction. [25] Closed-eye sign of medial lemniscus, also described with 4H leukodystrophy,[25] was also noted in our cohort, more commonly with PMD-like pattern (P value = 0.002) which also likely relates to delay in regional brainstem myelination. Some cases with the final MRI phenotype (washed-out pattern) demonstrated a greater T2 hyperintensity of the posterior limb of internal capsule and occipital lobe white matter than other regions, and delayed T1 peripheral cerebellar arborization. These again may correspond to regional specific delays in myelination persisting at advanced stages however it cannot be ruled out if a degree of gliosis with advancing age contributes to these signal changes. [8,28,34]

There are potential limitations in our study. There are drawbacks expected due to a retrospective study design including an inconsistent timing of MRI within the cohort. We could not address genotype correlations as data regarding the specific involved segment and/or gene haploinsufficiency was not available for many cases due to the retrospective nature of the study and would be desirable in future studies. Image acquisition parameters have been shown to influence myelination appearances, including magnet strength (1.5T vs 3T), type of sequences used (spin-echo Vs gradient recalled echo), type of spin echo sequence used (conventional Vs fast spin echo) and internal parameters (echo train length, TR, TE). [37–39] It was difficult to collect harmonized data as imaging protocols varied over the study period and also between the age-groups studied.

CONCLUSIONS

In conclusion, we systematically analyzed CNS imaging findings in a cohort of 18q abnormalities and found distinct MRI patterns corresponding to improving brain myelination. There were differences in MRI findings across the 18q subgroups with more severe white matter abnormalities in ring chromosome 18 and greater prevalence of structural abnormalities including small pons and vermis dimensions in trisomy 18. The findings in the cohort could represent an imaging continuum and larger studies are needed to validate this.

Table 1: Cohort Characteristics

Clinical Characteristics (n = 36)	
Age at first imaging (months)	19.6 (4.3 – 59.3)
Sex (F:M)	25:11 (2.2:1)
Diagnosis	18q deletion (18q-) - 23 (64)
	Trisomy 18 - 7 /Tetrasomy 18 – 1 (Total 8 (22))
	Ring chromosome 18 4 (11)
	18q inversion 1 (3)
Clinical Data	
Microcephaly*	13/19 (68)
Short Stature*	13/14 (93)
Visual impairment	11/15 (73)
Hearing impairment	9/15 (60)

Cleft palate	4/12 (33)
Epilepsy	8/18 (44)
Genitourinary	9/14 (64)
Cardiac	11/16 (69)
Imaging Characteristics (n = 50 MRIs)	
At least 1 Abnormal MRI	33/36 (92)
Abnormal white matter	35 (70)
Abnormal corpus callosum	30 (60)
Dysplastic/Agenetic CC	8 (16)
CC AP dimension <3rd centile*	18/47 (38)
Body and/or splenium thickness <3rd centile*	25/47 (53)
AP dimension pons <3rd centile*	10 (20)
CC dimension vermis <3rd centile*	14 (28)
Other findings	
Periventricular nodular heterotopia	3
Ectopic posterior pituitary	3
Holoprosencephaly variant (thickened lamina rostralis and fused fornices, SMMCI with PAS, absent olfactory bulbs), Aqueductal stenosis, Polymicrogyria	1 each

Table 2: Comparative analysis of the spectrum of imaging findings across the 18q chromosome abnormalities

	18q- group (n = 23)	Ring chromosome 18 group (n = 4)	Trisomy 18 group (Trisomy 18 n = 7, Tetrasomy 18 n = 1)	P value
Number of MRIs (n = 49)	34 (69)	5 (10)	10 (21)	-
Age at MRI	51.8 (17.8 – 114.4)	18.1 (14.9 – 212.2)	6.8 (0.17 – 43.7)	0.06
Abnormal white matter	25 (74)	5 (100)	5 (50)	0.11
Number of MRIs (n = 49)	34 (69)	5 (10)	10 (21)	-
Multifocal white matter hyperintensities	0	3 (60)	1 (10)	0.001 (18 ring vs others)
Myelination Patterns				
PMD-like pattern	4 (12)	1 (20)	2 (20)	0.37
Intermediate pattern	7 (21)	2 (40)	2 (20)	
Washed-out pattern	14 (41)	2 (40)	1 (10)	
Normal	9 (26)	0	5 (50)	
Myelination lag	17.2 (3.3 – 19.6)	27.0 (19.2 – 33.0)	9.0 (3.0 – 15.1)	0.005 (18 ring vs 18 trisomy) 0.03 (18 ring vs 18q-)
Biometric Measurements				
APD pons (mm)	18.5 (16.9 – 19.4)	15.3 (15.2 – 19.5)	13.0 (10.4 – 17.3)	0.002 (18 trisomy vs 18q-)
Pons APD <3rd centile	3 (9)	0 (0)	7 (70)	<0.001 (18 trisomy vs others)
Pons/FOD ratio	0.13 (0.12 – 0.14)	0.13 (0.12 – 0.14)	0.11 (0.10 – 0.12)	0.002 (18 trisomy vs 18q-) 0.02 (18 trisomy vs 18 ring)
CCD vermis (mm)	41.8 (37.1 – 45.7)	38.8 (36.8 – 43.5)	27.6 (19.4 – 35.0)	<0.001 (18 trisomy vs 18q-)
CCD vermis <3rd centile	7 (21)	0 (0)	7 (70)	0.003 (18 trisomy vs others)
CCD vermis/FOD ratio	0.30 (0.27 – 0.33)	0.31 (0.30 – 0.35)	0.23 (0.19 – 0.25)	<0.001 (18 trisomy vs 18q-) 0.002 (18 trisomy vs 18 ring)
TCD (mm)	88.4 (81.7 – 94.3)	78.2 (72.2 – 87.9)	63.9 (47.6 – 88.3)	0.04
TCD/FOD ratio	0.65 (0.59 – 0.68)	0.63 (0.59 – 0.72)	0.56 (0.49 – 0.63)	0.06

REFERENCES

1. Cody JD, Heard PL, Crandall AC, et al. Narrowing Critical Regions and Determining Penetrance for Selected 18q- Phenotypes. *Am J Med Genet A* 2009;149A:1421.

2. Heard PL, Carter EM, Crandall AC, et al. High Resolution Genomic Analysis of 18q− using oligo-microarray Comparative Genomic Hybridization (aCGH). *Am J Med Genet A* 2009;149A:1431–7.

3. Cody JD, Sebold C, Heard P, et al. Consequences of chromsome18q deletions. *Am J Med Genet C Semin Med Genet* 2015;169:265–80.

4. Cody JD, Heard P, Rupert D, et al. Chromosome 18 gene dosage map 2.0. *Hum Genet* 2018;137:961–70.

5. Cody JD, Hasi-Zogaj M, Heard P, et al. The Chromosome 18 Clinical Resource Center. *Mol Genet Genomic Med* 2018;6:416–21.

6. Feenstra I, Vissers LELM, Orsel M, et al. Genotype–phenotype mapping of chromosome 18q deletions by high-resolution array CGH: An update of the phenotypic map. *Am J Med Genet A* 2007;143A:1858–67.

7. Lancaster JL, Cody JD, Andrews T, et al. Myelination in Children with Partial Deletions of Chromosome 18q. *AJNR Am J Neuroradiol* 2005;26:447.

8. Loevner LA, Shapiro RM, Grossman RI, et al. White matter changes associated with deletions of the long arm of chromosome 18 (18q- syndrome): a dysmyelinating disorder? *AJNR Am J Neuroradiol* 1996;17:1843–8.

9. Inagaki M, Ando Y, Mito T, et al. Comparison of brain imaging and neuropathology in cases of trisomy 18 and 13. *Neuroradiology* 1987;29:474–9.

10. Norman RM. Neuropathological Findings in Trisomies 13–15 and 17–18 with Special Reference to the Cerebellum. *Dev Med Child Neurol* 1966;8:170–7.

11. Takano M, Hirata H, Kagawa Y, et al. Ratio of fetal anteroposterior to transverse cerebellar diameter for detection of the cerebellar hypoplasia in the second trimester and comparison with trisomy 18. *J Obstet Gynaecol Res* 2015;41:1757–61.

12. Fryns JP, Kleczkowska A, Jaeken J, et al. Mosaic 13 trisomy due to de novo 13/13 translocation with subsequent fission. Karyotype: 46,XX,-13, +t(13;13)(p11;q11)/46,XX,del(13)(p11). A second example. *Ann Genet* 1989;32:177–9.

13. Benini R, Saint-Martin C, Shevell MI, et al. Abnormal Myelination in Ring Chromosome 18 Syndrome. *J Child Neurol* 2012;27:1042–7.

14. Anzai M, Arai-Ichinoi N, Takezawa Y, et al. Patchy white matter hyperintensity in ring chromosome 18 syndrome. *Pediatr Int Off J Jpn Pediatr Soc* https://doi.org/10.1111/ped.13043.

15. Nakayama J, Hamano K, Shimakura Y, et al. Abnormal myelination in a patient with ring chromosome 18. *Neuropediatrics* 1997;28:335–7.

16. Ebrahimi-Fakhari D, Alecu JE, Ziegler M, et al. Systematic Analysis of Brain MRI Findings in Adaptor Protein Complex 4-Associated Hereditary Spastic Paraplegia. *Neurology* 2021;97:e1942–54.

17. Plecko B, Stöckler-Ipsiroglu S, Gruber S, et al. Degree of hypomyelination and magnetic resonance spectroscopy findings in patients with Pelizaeus Merzbacher phenotype. *Neuropediatrics* 2003;34:127–36.

18. Rutherford MA. *MRI of the Neonatal Brain*. W.B. Saunders; 2002.

19. Garel C, Cont I, Alberti C, et al. Biometry of the corpus callosum in children: MR imaging reference data. *AJNR Am J Neuroradiol* 2011;32:1436–43.

20. Jandeaux C, Kuchcinski G, Ternynck C, et al. Biometry of the Cerebellar Vermis and Brain Stem in Children: MR Imaging Reference Data from Measurements in 718 Children. *AJNR Am J Neuroradiol* 2019;40:1835–41.

21. Tich SNT, Anderson PJ, Hunt RW, et al. Neurodevelopmental and Perinatal Correlates of Simple Brain Metrics in Very Preterm Infants. *Arch Pediatr Adolesc Med* 2011;165:216–22.

22. Lee S, Lee DK. What is the proper way to apply the multiple comparison test? *Korean J Anesthesiol* 2018;71:353–60.

23. MacFarland TW, Yates JM. Wilcoxon Matched-Pairs Signed-Ranks Test. In: MacFarland TW, Yates JM, eds. *Introduction to Nonparametric Statistics for the Biological Sciences Using R*. Cham: Springer International Publishing; 2016:133–75.

24. Mayson TA, Ward V, Davies KR, et al. Reliability of retrospective assignment of gross motor function classification system scores. *Dev Neurorehabilitation* 2013;16:207–9.

25. Cayami FK, Bugiani M, Pouwels PJW, et al. 4H Leukodystrophy: Lessons from 3T Imaging. *Neuropediatrics* 2018;49:112–7.

26. Stricker T, Martin E, Boesch C. Development of the human cerebellum observed with high-field-strength MR imaging. *Radiology* 1990;177:431–5.

27. Kline AD, White ME, Wapner R, et al. Molecular analysis of the 18q- syndrome--and correlation with phenotype. *Am J Hum Genet* 1993;52:895–906.

28. Linnankivi T, Tienari P, Somer M, et al. 18q deletions: clinical, molecular, and brain MRI findings of 14 individuals. *Am J Med Genet A* 2006;140:331–9.

29. Gay CT, Hardies LJ, Rauch RA, et al. Magnetic resonance imaging demonstrates incomplete myelination in 18q- syndrome: evidence for myelin basic protein haploinsufficiency. *Am J Med Genet* 1997;74:422–31.

30. Malik P, Muthusamy K, Mankad K, et al. Solving the hypomyelination conundrum - Imaging perspectives. *Eur J Paediatr Neurol EJPN Off J Eur Paediatr Neurol Soc* 2020;27:9–24.

31. Kinoshita M, Nakamura Y, Nakano R, et al. Thirty-one autopsy cases of trisomy 18: clinical features and pathological findings. *Pediatr Pathol* 1989;9:445–57.

32. Weber WW, Mamunes P, Day R, et al. TRISOMY 17-18(E): STUDIES IN LONG-TERM SURVIVAL WITH REPORT OF TWO AUTOPSIED CASES. *Pediatrics* 1964;34:533–41.

33. Kakulas BA, Trowell HR, Cullity GJ, et al. The neuropathology of the 17-18 trisomy syndrome. *Proc Aust Assoc Neurol* 1968;5:189–95.

34. Vogel H, Urich H, Horoupian DS, et al. The Brain in the 18q- Syndrome. *Dev Med Child Neurol* 1990;32:732–7.

35. Felding I, Kristoffersson U, Sjöström H, et al. Contribution to the 18q- syndrome. A patient with del(18) (q22.3qter). *Clin Genet* 1987;31:206–10.

36. Whitehead MT, Raju A, Choudhri AF. Normal centrolineal myelination of the callosal splenium reflects the development of the cortical origin and size of its commissural fibers. *Neuroradiology* 2014;56:333–8.

37. Tyan AE, McKinney AM, Hanson T, et al. Comparison of spin-echo and gradient-echo T1-weighted and spin-echo T2-weighted images at 3T in evaluating term-neonatal myelination. *AJNR Am J Neuroradiol* https://doi.org/10.3174/ajnr.A4099.

38. Prenger EC, Beckett WW, Kollias SS, et al. Comparison of T2-weighted spin-echo and fast spin-echo techniques in the evaluation of myelination. *J Magn Reson Imaging JMRI* 1994;4:179–84.

39. Guleria S, Kelly TG. Myelin, myelination, and corresponding magnetic resonance imaging changes. *Radiol Clin North Am* 2014;52:227–39.

SUPPLEMENTAL FILES

Table 1. Region specific ICC coefficients for T1 and T2 scores across the two readers

T2 scores	ICC	95% CI	T1 Score	ICC	95% CI
MCP	0.86	0.76-0.92	MCP	0.87	0.77-0.92
BG	0.88	0.80-0.93	BG	0.84	0.72-0.91
Perirolandic Region	0.89	0.82-0.94	Perirolandic Cortex	0.77	0.59-0.87
PLIC	0.94	0.89-0.96	PLIC	0.85	0.73-0.91
Corona Radiata	0.86	0.76-0.92	Corona Radiata	0.90	0.82-0.94
Dorsal Pons	0.78	0.62-0.87	Dorsal Pons	0.91	0.85-0.95
Cerebellar White matter	0.92	0.86-0.95	Cerebellar WM	0.93	0.87-0.96
Optic Radiation	0.94	0.89-0.96	Optic Rad	0.89	0.82-0.94
Dentate Nucleus	0.90	0.83-0.94	Dentate Nucleus	0.90	0.82-0.94
Occipital Central WM	0.96	0.94-0.98	Occipital CWM	0.97	0.95-0.98
Splenium	0.92	0.87-0.95	Splenium	0.99	0.98-0.99
ALIC	0.89	0.81-0.94	ALIC	0.97	0.95-0.98
Occipital peripheral WM	0.98	0.96-0.98	Occipital PWM	0.92	0.86-0.95
Genu	0.87	0.78-0.93	Genu	0.99	0.98-0.99
Frontal Central WM	0.94	0.90-0.97	Frontal CWM	0.99	0.98-0.99
U-fibres	0.98	0.96-0.99	U-fibers	0.95	0.91-0.97
Frontal Peripheral WM	0.98	0.96-0.98	Frontal PWM	0.92	0.86-0.95
Periatrial WM	0.96	0.94-0.98	Centrum Semiovale	0.98	0.97-0.99
Total T2 score	0.98	0.97-0.99	Total T1 score	0.98	0.97-0.99

All p-values for ICC were <0.001

Table 2. MRI myelination phenotypes and comparative analysis

Myelination phenotypes		**PMD- like pattern**	**Intermediate pattern**	**Washed-out pattern**	**Normal white matter**	**P value**
Definition		Diffusely and homogenously T2 hyperintense white matter signal Preserved GWMD	Dirty/heterogenous white matter signal (dot-like appearance) Mixed areas of preserved and loss of GWMD	Better myelination with only milder T2 signal abnormality in the white matter Diffusely poor GWMD	Normal or near age-appropriate appearance of the white matter on T1 and T2 sequences	
Number of studies (%)	50	7 (14)	11 (22)	17 (34)	15 (30)	-
Age-range		9.9 (3-12)	22 (15.4 – 49)	113.6 (60.9 – 193.8)	45.3 (0.2 – 116.8)	<0.001 (Washed-out - PMD-like) 0.02 (Washed out - Intermediate) 0.01 (Washed-out – Normal)
$T2\ score_{avg}$	18 (12.8-20.6)	13 (12-15.2)	17 (13.75-18.7)	18 (16-19.7)	34.5 (8 – 35)	0.10
$T1\ score_{avg}$	33.2 (26.6 -	25 (16 – 27.5)	31.5 (29.7 – 34)	35.0 (33.5 -	35.0 (8.7 – 36)	0.01

	35.1)			35.5)		0.008 (PMD-like-Washed-out)
T1-T2 discordance (T1 $score_{avg}$ - T2 $score_{avg)}$	12 (1.0-16.1)	10 (2.5 – 12.7)	14 (12 – 17)	15.5 (14.5 – 17)	1 (0.7 – 1)	<0.001 (Normal – Washed-out) <0.001 (Normal – Intermediate)
Total myelination score	51.5 (40.0 - 55.2)	37 (30 – 41.2)	48 (44.7 – 52)	53 (52 – 54.5)	70 (16.7 – 71)	0.01 (PMD-like-Washed-out)
Myelination Lag	18.5 (16.0 – 22.5)	20 (10.2 – 22.2)	23 (18 – 25.2)	18 (16.5 – 19)	-	0.16
Corpus Callosum Abnormality	30 (60)	3 (43)	7 (64)	10 (59)	10 (67)	0.75
Corpus Callosum APD	54.6 mm (SD 10.3)	47.2 (SD 5.0)	52.2 (SD 11.9)	62.0 (SD 7.2)	50.2 (SD 8.7)	0.005 (Washed-out – PMD-like) 0.03 (Washed-out – Intermediate) 0.02 (Washed-out- Normal)
CCAPD/FOD ratio	0.414 (0.393 – 0.456)	0.408 (0.391 – 0.445)	0.417 (0.326 – 0.459)	0.447 (0.408 – 0.467)	0.404 (0.393 – 0.426)	0.12
Genu thickness	5.8 mm (SD 1.9)	4.2 (SD 0.7)	5.4 (SD 1.7)	6.9 (SD 1.7)	5.3 (SD 2.0)	0.01 (Washed-out - PMD)
Body thickness	3.4 mm (SD 1.1)	2.5 (SD 1.0)	3.6 (SD 1.0)	3.6 (SD 1.1)	3.7 (SD 1.3)	0.16
Splenium thickness	5.9 mm, (SD 2.5)	3.9 (SD 0.8)	5.5 (SD 1.8)	7.8 (SD 2.3)	4.6 (SD 1.7)	0.001 (Washed-out-PMD-like) 0.02 ((Washed-out-intermediate) 0.001 (Washed-out-normal)
Pons diameter	18.3 (15.2 – 19.2)	15.7 (13.6 – 17.7)	17.3 (15.7 – 18.7)	18.5 (18 – 19.2)	18.2 (12.2 – 19.9)	0.23
Pons/FOD ratio	0.132 (0.124 – 0.139)	0.133 (0.103 – 0.156)	0.131 (0.125 – 0.146)	0.130 (0.123 – 0.138)	0.134 (0.123 – 0.138)	0.91
Craniocaudal vermian diameter	40.3 (35.2 – 44.9)	35.9 (27.9 – 38.6)	41.9 (38.3 – 46.7)	43.8 (41.7 – 45.9)	35.3 (21.9 – 37.5)	0.01 (Washed-out – PMD-like) 0.001 (Normal – Washed-out) 0.02 (Normal – Intermediate)
CC Vermis/FOD ratio	0.297 (0.256 – 0.334)	0.304 (0.239 – 0.336)	0.340 (0.289 – 0.359)	0.315 (0.286 – 0.337)	0.272 (0.228 – 0.278)	0.009 (normal – washed-out) 0.001 (normal – intermediate)
Transverse cerebellar diameter (TCD)	87.1 (77.6 – 93.2)	73.8 (58.8 – 78.2)	85.3 (82.4 – 87.6)	91.7 (87.7 – 95.4)	88.9 (49.5 – 95)	0.003 (Washed-out – PMD-like)

TCD/FOD ratio	0.632 (0.587 – 0.684)	0.625 (0.548 – 0.655)	0.654 (0.595 – 0.669)	0.631 (0.615 – 0.690)	0.595 (0.502 – 0.688)	0.34
Closed eye sign Medial lemniscus	9 (18)	4 (66)	3 (33)	2 (13)	-	.002 (PMD-like vs washed-out pattern)
Focal T2 hyperintensity of mid splenium	3 (6)	1	1	1	-	0.65
Delayed peripheral T1 cerebellar arborization	26 (53, n = 49)	-	8 (100)	16 (94)	2 (13)	NA
Accentuated occipital lobe signal	6 (12)	-	-	6 (35)	-	NA
Accentuated PLIC signal extending to the central white matter	6 (12)	-	-	6 (35)	-	NA

Table 3. Expanded table for comparative analysis of the spectrum of imaging findings across the 18q chromosome abnormalities

	18q- group (23)	Ring chromosome 18 group (18 ring 4)	Trisomy 18 group (Trisomy 18 7, Tetrasomy 18 1)	P value
Number of MRIs (n = 49)	34 (69)	5 (10)	10 (21)	-
Age at MRI	51.8 (17.8 – 114.4)	18.1 (14.9 – 212.2)	6.8 (0.17 – 43.7)	0.06
Abnormal white matter	25 (74)	5 (100)	5 (50)	0.11
PMD-like pattern	4 (12)	1 (20)	2 (20)	0.37
Intermediate pattern	7 (21)	2 (40)	2 (20)	
Washed-out pattern	14 (41)	2 (40)	1 (10)	
Normal	9 (26)	0	5 (50)	
Myelination score	52.2 (47.3 – 56.1)	44 (36 – 51.7)	34 (17 – 55.2)	0.13
Myelination lag	17.2 (3.3 – 19.6)	27.0 (19.2 – 33.0)	9.0 (3.0 – 15.1)	0.005 (18 ring group vs 18 trisomy) 0.03 (18 ring vs 18q- group)
Multifocal white matter hyperintensities	0	3 (60)	1 (10)	0.001 (18 ring vs others)
Abnormal CC	20 (59)	2 (40)	7 (70)	0.53
Dysplastic/ agenetic	3 (9)	1 (20)	3 (30)	0.22
CC APD (mm)	55.8 (SD 8.9)	54.5 (SD 15.3)	49.3 (SD 12.5)	0.29
Genu thickness (mm)	5.8 (SD 1.5)	5.9 (SD 3.5)	5.0 (SD 2.0)	0.53
Body thickness (mm)	3.5 (SD 1.0)	4.3 (SD 1.6)	2.6 (SD 1.2)	0.03
Splenium thickness (mm)	6.0 (SD 1.8)	7.4 (SD 5.0)	4.5 (SD 2.5)	0.12
Fronto-occipital diameter (FOD, mm)	136.3 (122.5 – 143.6)	118 (108.3 – 138.9)	109.2 (95.9 – 140.1)	0.32
Pons dimension (mm)	18.5 (16.9 – 19.4)	15.3 (15.2 – 19.5)	13.0 (10.4 – 17.3)	0.002 (18 trisomy group vs 18q- group)
Pons APD <3rd centile	3 (9)	0 (0)	7 (70)	<0.001 (18 trisomy vs others)
Pons/FOD ratio	0.135 (0.127 – 0.141)	0.136 (0.129 – 0.149)	0.112 (0.103 – 0.128)	0.002 (18 trisomy

				group vs 18q- group) 0.02 (18 trisomy group vs 18 ring group)
CC Vermis (mm)	41.8 (37.1 – 45.7)	38.8 (36.8 – 43.5)	27.6 (19.4 – 35.0)	<0.001 (18 trisomy group vs 18q- group)
CC Vermis <3rd centile	7 (21)	0 (0)	7 (70)	0.003 (18 trisomy vs others)
CC Vermis/FOD ratio	0.308 (0.275 – 0.339)	0.315 (0.308 – 0.354)	0.233 (0.194 – 0.255)	<0.001 (18 trisomy group vs 18q- group) 0.002 (18 trisomy group vs 18 ring group)
Transverse cerebellar diameter (TCD, mm)	88.4 (81.7 – 94.3)	78.2 (72.2 – 87.9)	63.9 (47.6 – 88.3)	0.04 (18 trisomy group vs 18q- group)
TCD/FOD ratio	0.651 (0.593 – 0.689)	0.635 (0.598 – 0.724)	0.565 (0.494 – 0.638)	0.06

Table 4. Comparison of 18q cohort with age and sex matched controls

	18q combined (50)	Controls (100)	P value
CC APD (mm)	55.6 (SD 9.1)	61.6 (SD 10.1)	<0.001
Genu thickness (mm)	5.7 (SD 1.6)	8.8 (SD 2.5)	<0.001
Body thickness (mm)	3.3 (SD 1.1)	4.9 (SD 1.4)	<0.001
Splenium thickness (mm)	5.9 (SD 2.0)	8.4 (SD 2.6)	<0.001
Fronto-occipital diameter (FOD, mm)	134.5 (117.8 – 141.2)	148.1 (136.5 – 159.5)	<0.001
CC APD/FOD ratio	0.414 (0.393 – 0.456)	0.428 (0.406 – 0.446)	0.36
Pons dimension (mm)	18.5 (16.5 – 19.3)	19.6 (17.6 – 21.6)	<0.001
Pons/FOD ratio	0.132 (0.124 – 0.139)	0.133 (0.127 – 0.140)	0.06
CC Vermis (mm)	40.3 (35.2 – 44.9)	41.9 (37.8 – 45.6)	0.001
CC Vermis/FOD ratio	0.297 (0.256 – 0.334)	0.279 (0.258 – 0.297)	0.44
Transverse cerebellar diameter (TCD, mm)	87.1 (77.6 – 93.2)	96.9 (90.4 – 102.0)	<0.001
TCD/FOD ratio	0.632 (0.587 – 0.684)	0.639 (0.602 – 0.664)	0.09

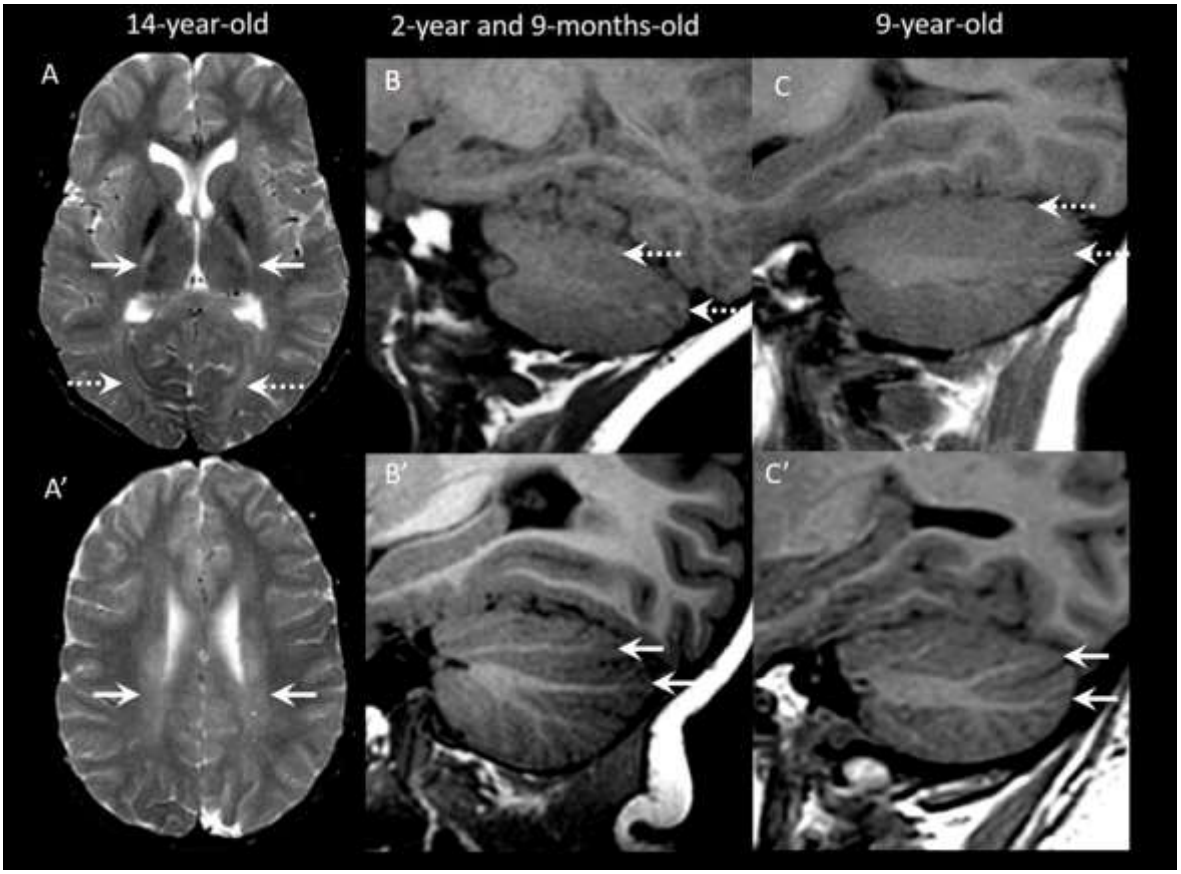

Supplementary Fig 1. Accentuated signal PLIC, occipital lobes and delayed T1 cerebellar arborization. Axial T2 images in a 14-year-old show hyperintensity of the PLIC and the adjacent central white matter (solid arrows A,A') and hyperintensity of the occipital lobe white matter (dashed arrows, in comparison to the frontal lobe white matter denoted by asterisk). T1 sagittal images at the level of the trigone (B,C) show poor definition and thickness of the peripheral cerebellar white matter stripes (dashed arrows, B,C). Age-matched controls in the lower panels (B',C') for reference.